Caenorhabditis elegans AF4/FMR2 Family Homolog *affl-2* Regulates Heat-Shock-Induced Gene Expression

Sophie J. Walton,* Han Wang,*,[1] Porfirio Quintero-Cadena,* Alex Bateman,[†] and Paul W. Sternberg*,[2]
*Division of Biology and Biological Engineering, California Institute of Technology, Pasadena, California 91125 and [†]European Molecular Biology Laboratory, European Bioinformatics Institute, (EMBL-EBI), Wellcome Genome Campus, Hinxton, Cambridge CB10 1SD, United Kingdom

ORCID IDs: 0000-0003-1320-1525 (S.J.W.); 0000-0002-1933-5762 (H.W.); 0000-0003-0067-5844 (P.Q.-C.); 0000-0002-6982-4660 (A.B.); 0000-0002-7699-0173 (P.W.S.)

ABSTRACT To mitigate the deleterious effects of temperature increases on cellular organization and proteotoxicity, organisms have developed mechanisms to respond to heat stress. In eukaryotes, HSF1 is the master regulator of the heat shock transcriptional response, but the heat shock response pathway is not yet fully understood. From a forward genetic screen for suppressors of heat-shock-induced gene expression in *Caenorhabditis elegans*, we found a new allele of *hsf-1* that alters its DNA-binding domain, and we found three additional alleles of *sup-45*, a previously molecularly uncharacterized genetic locus. We identified *sup-45* as one of the two hitherto unknown *C. elegans* orthologs of the human AF4/FMR2 family proteins, which are involved in regulation of transcriptional elongation rate. We thus renamed *sup-45* as *affl-2* (AF4/FMR2-Like). Through RNA-seq, we demonstrated that *affl-2* mutants are deficient in heat-shock-induced transcription. Additionally, *affl-2* mutants have herniated intestines, while worms lacking its sole paralog (*affl-1*) appear wild type. AFFL-2 is a broadly expressed nuclear protein, and nuclear localization of AFFL-2 is necessary for its role in heat shock response. *affl-2* and its paralog are not essential for proper HSF-1 expression and localization after heat shock, which suggests that *affl-2* may function downstream of, or parallel to, *hsf-1*. Our characterization of *affl-2* provides insights into the regulation of heat-shock-induced gene expression to protect against heat stress.

KEYWORDS *affl-1*; *affl-2*; heat shock response; *C. elegans*; AF4/FMR2

HEAT is a universal source of stress in nature, and temperature increases have detrimental effects, including disrupting cellular organization and proteostasis (Morimoto 1998). Upon heat stress, rapid transcriptional changes occur to upregulate genes that assist with restoring homeostasis (Morimoto 1998; Hajdu-Cronin *et al.* 2004; Richter *et al.* 2010). HSF1 has been identified as the primary regulator of heat-shock-induced transcription in eukaryotes (Åkerfelt *et al.* 2010; Richter *et al.* 2010). The current model for transcriptional control of heat shock response by HSF1 is as follows: under normal conditions, chaperones sequester HSF1, but, upon heat stress, the chaperones disassociate from HSF1, making it free to upregulate other genes (Voellmy and Boellmann 2007; Richter *et al.* 2010). However, the complete regulatory system that is responsible for the precise transcriptional control of heat shock response is not yet fully understood (Richter *et al.* 2010).

RNA polymerase II can become paused at the promoter-proximal region after initiation, and escape from the paused state can be a rate-limiting process in transcription (Kuras and Struhl 1999; Sims *et al.* 2004; Saunders *et al.* 2006; Levine 2011; Lin *et al.* 2011; Luo *et al.* 2012a; Zhou *et al.* 2012). In metazoans, positive transcription elongation factor beta (P-TEFb)—a heterodimeric kinase complex composed of CDK-9 and a Cyclin T1 partner—phosphorylates RNA Polymerase II and associated factors to stimulate promoter escape (Lenasi and Barboric 2010; Levine 2011; Luo *et al.* 2012b; Zhou *et al.* 2012). When performing this function, P-TEFb participates in the super elongation complex (SEC): a multi-subunit complex composed of a P-TEFb, an AF4/FMR family protein (AFF1 or AFF4), a Pol II elongation factor (ELL1, ELL2, or ELL3), a partner protein (EAF1 or EAF2), and an ENL family protein (ENL or AF9) (Lin *et al.*

doi: https://doi.org/10.1534/genetics.120.302923
Manuscript received October 21, 2019; accepted for publication May 27, 2020; published Early Online June 9, 2020.
Supplemental material available at: https://doi.org/10.22002/d1.1302.
[1]Present address: Department of Integrative Biology, University of Wisconsin-Madison, Madison, WI 53706.
[2]Corresponding author: Division of Biology and Biological Engineering, California Institute of Technology, Mail Code 156-29, 1200 E. California Blvd., Pasadena, CA 91125. E-mail: pws@caltech.edu

2010; Luo *et al.* 2012b). As in other metazoans, RNA polymerase II pausing occurs in *Caenorhabditis elegans* (Baugh *et al.* 2009; Maxwell *et al.* 2014), and *C. elegans* has been used as a multicellular *in vivo* model to perform genetic analysis of homologs of components of the SEC. However, a *C. elegans* version of the AF4/FMR2 family proteins, which serve as the scaffolds for the SEC, has not yet been identified.

Forward genetic screens are powerful methods to identify genes involved in a biological process. *hsf-1*, the gene encoding the sole ortholog of human HSF1 in *C. elegans*, was cloned in a forward genetic screen for suppressors of activated GOA-1 under the control of the *hsp-16.2* heat-shock promoter (Hajdu-Cronin *et al.* 2004). In addition to regulating heat-shock-induced transcription (Hajdu-Cronin *et al.* 2004; Brunquell *et al.* 2016), *hsf-1* plays roles in a diverse set of processes including development, aging, and immunity (Hsu *et al.* 2003; Hajdu-Cronin *et al.* 2004; Morley and Morimoto 2004; Dai *et al.* 2007; Li *et al.* 2017). The many distinct roles of *hsf-1* suggest that understanding heat-shock response can potentially provide insight into more general stress response pathways. *sup-45*, was identified in the same forward genetic screen as *hsf-1*, and shown to be necessary for heat-shock-induced *hsp-16.2* expression, but *sup-45* was not cloned (Hajdu-Cronin *et al.* 2004).

In a genetic screen for suppressors of heat-shock-induced gene expression, we identified a new reduction of function *hsf-1* allele and three new alleles of *sup-45*. We cloned *sup-45* and found that it is an AF4/FMR2 homolog, so we renamed *sup-45* as *affl-2* (AF4/FMR2-Like). *affl-2* encodes a previously uncharacterized protein that is predicted to have two nuclear localization signals and a collection of disordered residues at its N terminus. Through RNA-seq, we demonstrated that *affl-2* mutants are deficient in heat-shock-induced gene expression, which indicates that AFFL-2 regulates transcription in response to heat shock. In addition to being defective in heat-shock response, some *affl-2* mutants have intestines protruding from their vulvae. We found that AFFL-2 is a broadly expressed nuclear protein, and its nuclear localization is necessary for its role in heat-shock response. *affl-2* is not necessary for the proper localization and expression of HSF-1 pre or post heat shock, suggesting that *affl-2* may function downstream of *hsf-1*. Our identification and characterization of *affl-2* advances our understanding of heat-shock response induced transcriptional regulation in *C. elegans*.

Materials and Methods

C. elegans cultivation

C. elegans were grown using the methods described in Brenner (1974). Strains were maintained on NGM agar plates at room temperature (20°) and fed OP50, a slow-growing strain of *Escherichia coli*. A list of strains used in this study can be found in Supplementary Experimental Procedures.

Genomic editing

We made *affl-1* mutants by inserting the STOP-IN cassette in the 5′ end of the coding sequence of *affl-1* using CRISPR/Cas9 with a coconversion marker (Wang *et al.* 2018). We injected N2 worms to create *affl-1 (sy1202)* single mutants, and we injected *affl-2(sy975)* worms to create *affl-2(sy975) affl-1(sy1220)* double mutants. *sy1202* and *sy1220* had the same molecular change in the *affl-1* gene. The sequence change is a 43 bp insertion with 3-frame stop codons and is near the 5′ end of the coding sequence of *affl-1*:

5′ flanking seq: CCGTACCCGTAGAATGCTTGAAGAAATGGCCG GCC
43 bp insertion: GGGAAGTTTGTCCAGAGCAGAGGTGACTAA GTGATAA
3′ flanking seq: TCGTGGGAACTAAACCATTGAGCCAGCTTCC TCGAAG

Primers for genotyping and sequencing can be found in the Supplementary Experimental Procedures.

Generation of transgenic lines

Methods to generate transgenic animals were adapted from Mello and Fire (1995). The *affl-2* driver strain was constructed by injecting 25 ng/μl of pSJW003 along with 40 ng/μl of P*unc-122*::*rfp* and 35 ng/μl of 1 kb DNA ladder (NEB) into the GFP effector strain *syIs300*, and then outcrossing the resulting worms to add the GFP::H2B effector strain *syIs407* in place of *syIs300* (Wang *et al.* 2017). All *affl-2* rescue variants were constructed by injecting 10 ng/μl of the plasmid containing the rescue construct along with 80 ng/μl of pBluescript and 10 ng/μl of the co-injection marker plasmid KP1368 (P*myo-2*::*nls*::*mCherry*) into the strain PS8082 [*syIs231 II*; *affl-2 (sy975) III*]. A list of transgenic lines and plasmids used can be found in the Supplementary Experimental Procedures.

lin-3c overexpression assays

We used pumping quiescence as a readout for expression of heat-shock driven *lin-3c*, for cessation of pumping is characteristic of *lin-3c* overexpression induced quiescence. We adapted our *lin-3c* overexpression assay from that of Van Buskirk and Sternberg (2007). 15–30 L4 animals were picked onto NGM agar plates that were seeded 48–72 hr prior; 16–20 hr later, plates with adult animals were covered with parafilm and placed in a 33° water bath for 15 min. We used a 15-min heat shock rather than a 30-min heat shock because we wanted to be able to detect weaker suppressors. Plates were then left in 20° with their lids open to recover for 3 hr before scoring for pumping quiescence. By this time, all worms would have recovered from the mild heat shock, and would thus exhibit only *lin-3c* overexpression dependent quiescence. Pumping quiescence was scored using a stereomicroscope on 25–50× magnification, and quiescence was defined as a cessation of movement of the pharyngeal bulb.

Herniated intestine quantification

We synchronized adults for each genotype by picking ~30 L4 animals onto NGM agar plates 20–24 hr prior to the assay. We then counted the number of adults with a visible loose piece

of tissue near their vulva using a stereomicroscope on 25–50× magnification.

Isolation of suppressors

Ethyl methanesulfonate mutagenesis: Mutagenesis was performed on ~500 late L4 hermaphrodites (PS7244) as described by Brenner (1974). In particular, worms were incubated in a solution of 4 ml M9 with 20 μl Ethyl methanesulfonate (EMS; Sigma) for 4 hr. At the end of the 4 hr, we washed the worms three times each with 3 ml of M9 to dilute the EMS. We then plated the mutagenized worms on a seeded NGM agar plate outside the OP50 lawn and left them to recover for at least 30 min before plating the P0 worms.

To screen a synchronized F_2 population, we treated the F_1 adults with alkaline hypochlorite (bleach) treatment to isolate the eggs of the F_2 generation (Protocol B from Porta-de-la-Riva *et al.* 2012). After bleaching treatment, we immediately plated the F_2 generation eggs. These steps ensured that all of our F_2 animals reached adulthood at roughly the same time.

We performed the *lin-3c* overexpression assay as described above on adult F_2 worms. We isolated worms who did not exhibit pumping quiescence onto separate plates, and we screened their progeny (F_3 generation) to ensure that the phenotype was stable. Mutants isolated from different P_0 plates were deemed independent.

Dominance tests and complementation tests with hsf-1 and affl-2 mutants: To identify *hsf-1* and *affl-2* mutants, we performed complementation tests with *hsf-1(sy441)*, *affl-2(sy509)*, and *affl-2(sy978)* mutants. Note that *affl-2* was originally named *sup-45*. For each complementation test, one allele was crossed into *syIs197(hs:lin-3c)*; *him-5* males, and homozygous males were then crossed into hermaphrodites of a second strain. For tests of dominance, we performed crosses using *syIs197* males. Either mutant *syIs197* males were crossed into a wild-type background, or wild-type *syIs197* males were crossed into a mutant background. We performed the *lin*-3c overexpression assay on F_1 cross progeny of the crosses to assay dominance.

SNP mapping: We used the polymorphic Hawaiian strain CB4856 to perform SNP mapping of our suppressor loci (Doitsidou *et al.* 2010). Our SNP mapping strain was PS7421, which we created by outcrossing PS7244 10 times to CB4856. We followed the Hobert laboratory's protocol for worm genomic DNA preparation for SNP mapping (pooled samples). For each suppressor, genomic DNA from the progeny of 50 suppressors and 50 nonsuppressors crossed with PS7421 were collected. For identifying Y55B1BR.2 we sequenced PS75971 [*syIs231 II*; *affl-2(sy978) III*] crossed into PS7421 (Hawaiian strain) and searched for regions where the rate of recombination was low (see Supplemental Material, Figure S1). We also directly sequenced PS8082 [*syIs231 II*; *affl-2 (sy975) III*] in an N2 background. We analyzed our sequencing results using MiModD mapping software to identify putative mutations (Maier *et al.* 2014).

Protein sequence analysis

Y55B1BR.2 similarity to AF4 was found in the first iteration of a JackHMMER iterative search on the EMBL-EBI webserver (Potter *et al.* 2018). Further rounds of searching revealed homologs in a wide range of eukaryotic species. The search was performed against Reference Proteomes using the phmmer algorithm with the following settings:

HMMER Options: -E 1--domE 1--incE 0.01--incdomE 0.03--mx BLOSUM62--pextend 0.4--popen 0.02--seqdb uniprotrefprot

We used the MUSCLE alignment tool with the default settings to create multiple sequence alignments (Edgar 2004). The alignment of the C-terminal homology domain (CHD) was generated using the MUSCLE alignment tool on a selected set of 16 eukaryotic homologs identified using JackHMMER (Edgar 2004).

To determine the location of the predicted nuclear localization signals (NLSs) we used the cNLS mapper with a cut-off score of 0.5 and the option to search for bipartite NLSs with a long linker within terminal 60-amino-acid regions (Kosugi *et al.* 2008; 2009a,b). We checked that these predictions were consistent with PSORT and NucPred (Nakai and Horton 1999; Brameier *et al.* 2007). We used IUPred2A long disorder (Dosztányi *et al.* 2005, 2018) to predict disordered regions of AFFL-2, AFFL-1, AFF1, and AFF4. We used ANCHOR2 software to predict the presence of the disordered protein binding regions of AFFL-2, AFFL-1, AFF1, and AFF4 (Dosztányi *et al.* 2009, 2018).

Molecular biology

We used Roche Taq for genotyping PCR products <1 kb, and we used NEB Phusion High Fidelity or NEB High Fidelity Q5 for PCR of all cloning inserts and genotyping PCR products >1 kb. NEB T4 Ligase was used to construct pSJW003. The NEBuilder HiFi DNA Assembly Master Mix was used for Gibson Assembly of pSJW005, pSJW035, pSJW036, pSJW040, and pSJW041. We used DH5α competent cells for all transformations, and we plated all transformed cells on carbenicillin LB plates. A detailed list of oligonucleotides and plasmids can be found in the Supplementary Experimental Procedures.

Microscopy

Images of whole worm phenotypes were taken using a Plan Apochromat 10x DIC objective in a Zeiss Imager Z2 microscope with an Axiocam 506 Mono camera using ZEN Blue 2.3 software. Worms were synchronized by picking L4s were picked 20–24 hr prior to imaging, and worms were anesthetized in 3 mM levamisole and mounted on 2% agarose pads.

Images of *affl-2* expression and localization of HSF-1::GFP and AFFL-2::GFP were taken using a Plan Apochromat 10x or 63x/1.4 Oil DIC objective in a Zeiss Imager Z2 microscope with an Axiocam 506 Mono camera using ZEN Blue 2.3 software. Young adults were used for imaging, because their

lower fat content made it easier to detect fluorescent proteins. Worms were anesthetized in 3 mM levamisole and mounted on 2% agarose pads. Z-stacks were taken at 63x and maximum-intensity projections were generated using Fiji/ImageJ software (Schindelin *et al.* 2012). Z-stacks were used for images of HSF-1::GFP localization, and, when indicated, for AFFL-2::GFP localization.

Our method to image HSF-1::GFP was adapted from Morton and Lamitina (2013). To image HSF-1::GFP after heat shock, worms were mounted on slides and placed in foil packets on top of wells in a preheated PCR machine at 35° for 5 min. We found that a 5-min heat shock was long enough to cause worms to form granules consistently, and longer incubation caused the plates to dry out. Worms were imaged immediately after heat shock. Nonheat shock controls were left on the benchtop (20°) for 5 min prior to imaging. In our image analysis, we selected nuclei manually, and chosen nuclei were segmented automatically. We detected granules in chosen nuclei automatically using the blob detector function from scikit-image (van der Walt *et al.* 2014). We used the mean intensity of the segmented nuclei and granules after background subtraction to determine HSF-1::GFP nuclear intensity.

To image AFFL-2::GFP after heat shock, worms were heat shocked following the same protocol as we used for the *lin-3c* overexpression assay. We choose to use this protocol rather than the one adapted from Morton and Lamitina (2013) because we wanted to recreate the conditions of the worms were in during the genetic screen. After the heat shock, worms were immediately mounted onto slides and imaged.

Data analysis

Unless otherwise specified, data analysis was carried out using Python 3.7 with standard scientific libraries (Jones *et al.* 2001) and version 0.041 of the bebi103 package (Bois 2018).

Determining probability parameters: Since we collected data from a few trials on different days, our experiments have a hierarchical structure. Therefore, we decided to use Bayesian hierarchical models to estimate all probabilities. Our methods are based on those documented in Bois (2018). Briefly, we describe our general model for each experiment.

For each experiment, our goal is to estimate master parameter ϕ, which is the probability of an animal exhibiting a certain phenotype. However, for each trial, the probability of a worm exhibiting a phenotype may be slightly different due to day-to-day variations. Thus, the probability of a worm exhibiting a phenotype in trial i is θ_i rather than ϕ. For a given trial, i, of N_i animals, the we model n_i, the number of animals that exhibit a given phenotype, as binomially distributed:

$$n_i \sim Binomial\,(N_i,\, \theta_i)$$

To specify the full generative model, we must specify our hyperprior for ϕ and our priors for θ_i. Our hyperprior for ϕ is

$$\phi \sim Beta\,(\alpha_h,\, \beta_h)$$

To make the prior uniformative, we choose $\alpha_h = 1$, $\beta_h = 1$ which is equivalent to a uniform distribution from $[0, 1]$. We model each θ_i as varying from ϕ as follows:

$$\kappa \sim Halfnorm\,(\sigma)$$

$$\alpha = \phi\kappa$$

$$\beta = (1-\phi)\kappa$$

$$\theta_i \sim Beta(\alpha, \beta)$$

We choose $\sigma = 30$. Thus our full generative model is as follows:

$$\phi \sim Beta\,(1, 1)$$

$$\kappa \sim Halfnorm\,(30)$$

$$\alpha = \phi\kappa$$

$$\beta = (1-\phi)\kappa$$

$$\theta_i \sim Beta(\alpha, \beta)$$

And our likelihood for our data, n_i is

$$n_i \sim Binomial\,(N_i,\, \theta_i)$$

We used Stan to sample from the posterior distribution of ϕ and report credible intervals for ϕ (Stan Development Team 2018).

Quantification of HSF-1 expression and nuclear granule formation: We used nonparametric bootstrapping to estimate the median of the number of granules per nuclei formed, the mean intensities of HSF-1::GFP nuclei prior to heat shock, and the mean intensities of HSF-1::GFP nuclear granules after shock in each strain.

RNA-seq

RNA preparation for RNA-seq: We followed the heat shock protocol for RNA-seq as described in Brunquell *et al.* (2016). For each condition in each replicate, we picked 250 L4s onto plates freshly seeded with OP50. To heat shock worms, we covered each plate with parafilm and placed it in a preheated water bath at 33° for 30 min. For the nonheat shock condition, we covered each plate with parafilm and left it at room temperature (20°) for 30 min.

After heat shock, worms were immediately washed off of plates using M9 and rinsed three times before being frozen in liquid N2. Worms were lysed using a mortar and pestle, and RNA was extracted using Qiagen's RNeasy kit.

cDNA libraries were made and RNA-sequencing was performed at the Mildred and Muriel Genomics Laboratory at

Caltech. RNA integrity was assessed using RNA 6000 Pico Kit for Bioanalyzer (#5067-1513; Agilent Technologies), and mRNA was isolated using NEBNext Poly(A) mRNA Magnetic Isolation Module (#E7490; NEB). RNA-seq libraries were constructed using NEBNext Ultra II RNA Library Prep Kit for Illumina (#E7770; NEB) following the manufacturer's instructions. Briefly, mRNA isolated from ~200 ng–1 μg of total RNA was fragmented to the average size of 200 nt by incubating at 94° for 15 min in first-strand buffer, cDNA was synthesized using random primers and ProtoScript II Reverse Transcriptase followed by second-strand synthesis using NEB Second Strand Synthesis Enzyme Mix. Resulting DNA fragments were end-repaired, dA tailed, and ligated to NEBNext hairpin adaptors (#E7335; NEB). After ligation, adaptors were converted to the "Y" shape by treating with USER enzyme, and DNA fragments were size selected using Agencourt AMPure XP beads (#A63880; Beckman Coulter) to generate fragment sizes between 250 and 350 bp. Adaptor-ligated DNA was PCR-amplified followed by AMPure XP bead clean up. Libraries were quantified with Qubit dsDNA HS Kit (#Q32854; ThermoFisher Scientific), and the size distribution was confirmed with High Sensitivity DNA Kit for Bioanalyzer (#5067- 4626; Agilent Technologies). Libraries were sequenced on Illumina HiSeq2500 in single-read mode with the read length of 50 nt to a depth of 20 million reads per sample following manufacturer's instructions. Base calls were performed with RTA 1.13.48.0 followed by conversion to FASTQ with bcl2fastq 1.8.4.

RNA-seq data analysis: RNA-seq quantification was performed with Kallisto (Bray *et al.* 2016) version 0.44 using 200 bootstraps in single-end mode, average length of 300 bp, SD of 20 bp, and a transcriptome index built from genome assembly WBcel235. All statistical analysis was conducted in R (3.6.1) using Sleuth (0.30.0) (Pimentel *et al.* 2017). All plots were created using custom scripts in Python (3.7).

Data availability

Strains and plasmids are available upon request. Code for data analysis and image processing can be found at: https://github.com/sophiejwalton/affl-2.git. The GEO accession number for RNA-sequencing data is: GSE151164. Other data and supplementary material can be found at: https://doi.org/10.22002/d1.1302.

Results

A suppressor screen of hsp-16.41:lin-3c-induced pumping quiescence yields new alleles involved in heat-shock-induced gene expression

We conducted a forward genetic screen to search for suppressors of pumping quiescence caused through P*hsp-16.41* (promoter of *hsp-16.41*)-driven *lin-3c* overexpression (Figure 1A). When overexpressed in adult animals, the *lin-3c* isoform of *lin-3*, which encodes the *C. elegans* ortholog of the epidermal growth factor (EGF), causes a reversible state of quiescence that is characterized by decreased responsiveness, along with cessation of pumping, locomotion, and defecation (Van Buskirk and Sternberg 2007). Expression of *hsp-16.41* is induced by heat shock; therefore, placing *lin-3c* under the control of P*hsp-16.41* gives us temporal control of quiescence. We screened for suppressors of *lin-3c*-induced pumping quiescence in order to find mutants that are defective in downstream steps of quiescence or do not express the *lin-3c* transgene properly (Figure 1A). The gene *hsf-1* was identified from a similar screen using a transgene with a gain-of-function *goa-1* driven by the promoter of *hsp-16.2*, another heat-shock response gene similar to *hsp-16.41* (Hajdu-Cronin *et al.* 2004). We found one of the strong recessive suppressors, *sy1198*, failed to complement *hsf-1(sy441)* for suppression of *lin-3c* overexpression induced quiescence, which indicated that *sy1198* is an allele of *hsf-1* (Table S1 and S2). By Sanger sequencing, we found *sy1198* is a T to A mutation in the *hsf-1* gene, which leads to a leucine to glutamine substitution (L93Q) in the predicted DNA binding domain of HSF-1 protein (Figure 1B and Table 1). As null mutants of *hsf-1* are lethal (Li *et al.* 2016), *sy1198* is likely to be a weak loss-of-function allele.

Among the suppressors, we identified three alleles (*sy975*, *sy981*, and *sy978*) that failed to complement (Table S2). *sy978* was mapped to the left tip of Chr III (Figure S1), which is the same region of that of *sup-45*, an uncloned gene reported to be involved in heat-shock-induced gene expression (Hajdu-Cronin *et al.* 2004). Additionally, we found that *sup-45(sy509)* and *sy978* fail to complement. We confirmed that both *sup-45* alleles from Hajdu-Cronin *et al.* (2004) (*sy509* and *sy439*) and the three we identified (*sy981*, *sy978*, *sy975*) contain mutations in Y55B1BR.2 (Table 1 and Figure 1D), which we renamed as *affl-2* (see below for reasoning). For the rest of our experiments, we used *sy975*, which contains a nonsense mutation at residue 456 (Figure 1, C and D and Table 1), because we had outcrossed the strain four times and did not observe significant differences in phenotypes between the different alleles.

affl-2 mutants have herniated intestines and are deficient in heat-shock-induced transgene expression

We found that AFFL-2 has an adjacent paralog, Y55B1BR.1, whose encoding gene has a start codon that is separated from the stop codon of Y55B1BR.2 by only 489 nucleotides ("Y55B1BR.2 (gene)—WormBase: Nematode Information Resource). We thus renamed Y55B1BR.1 as AFFL-1. We did not find any *affl-1* mutants in our screen, so we made a putative null mutant of *affl-1* and an *affl-2(sy975) affl-1(sy1220)* double-mutant. *affl-2* mutants have been found to be Egl (EGg Laying defect) and Dpy (Dumpy) (Hajdu-Cronin *et al.* 2004). We also noticed that some *affl-2* mutants have their intestines protruding from their vulvas (Figure 2B). *affl-1* mutants appear wild type, and *affl-2(sy975) affl-1(sy1220)* double-mutant animals have the same morphological defects as *affl-2(sy975)* single mutants (Figure S2).

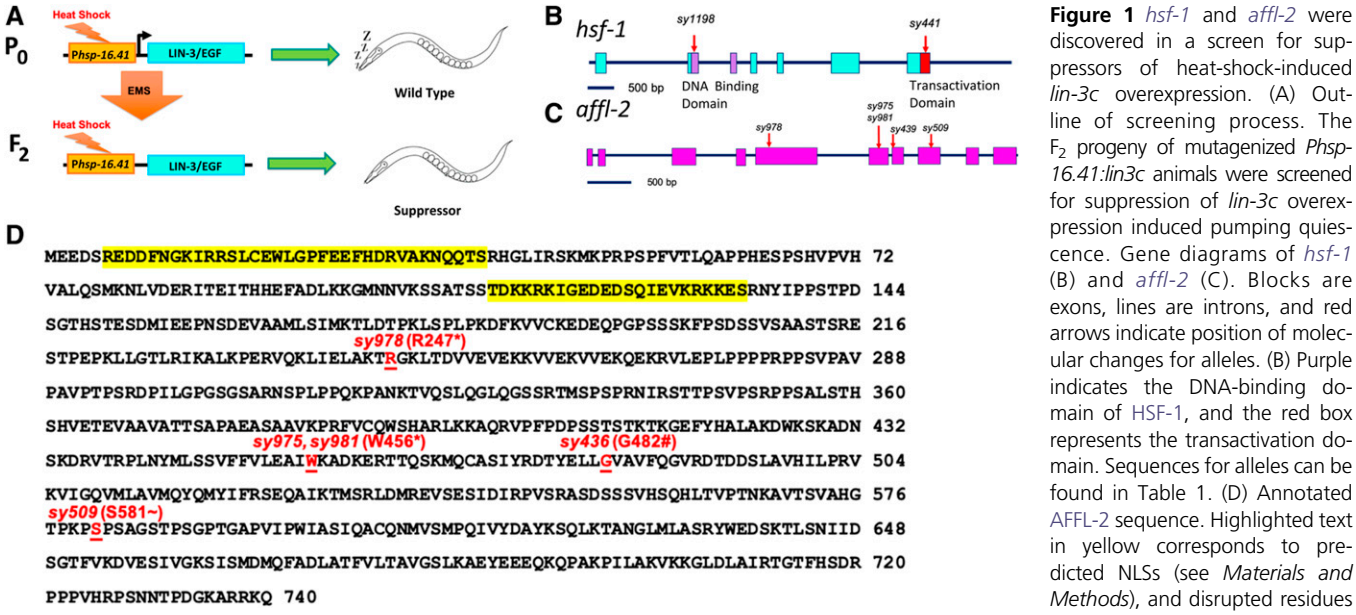

Figure 1 *hsf-1* and *affl-2* were discovered in a screen for suppressors of heat-shock-induced *lin-3c* overexpression. (A) Outline of screening process. The F_2 progeny of mutagenized *Phsp-16.41:lin3c* animals were screened for suppression of *lin-3c* overexpression induced pumping quiescence. Gene diagrams of *hsf-1* (B) and *affl-2* (C). Blocks are exons, lines are introns, and red arrows indicate position of molecular changes for alleles. (B) Purple indicates the DNA-binding domain of HSF-1, and the red box represents the transactivation domain. Sequences for alleles can be found in Table 1. (D) Annotated AFFL-2 sequence. Highlighted text in yellow corresponds to predicted NLSs (see *Materials and Methods*), and disrupted residues due to allele change are underlined in red text. * indicates nonsense mutation; # indicates splice site disruption prior to residue; ~ indicates first disrupted residue of missense mutation and frameshift caused by *sy509*.

Previous research has demonstrated that *hsf-1* is necessary for heat-shock-induced *hsp-16.41* expression (Hajdu-Cronin *et al.* 2004; Brunquell *et al.* 2016), and we also showed that *affl-2* mutants have diminished heat-shock-induced *hsp-16.41* transcription (see below). Thus, *affl-2* and *hsf-1* mutants are defective in quiescence due to *hsp-16.41*-driven *lin-3c* overexpression because they are unable to express the transgene properly. We decided to use heat-shock inducible pumping quiescence, due to expression of *Phsp-16.41*-driven *lin-3c* as a readout for *hsp-16.41* expression. We estimated ϕ, the probability of a given worm pumping after heat shock, to see whether the *hsp-16.41* promoter is active under heat shock conditions in *affl-2*, *hsf-1*, *affl-1*, and *affl-2 affl-1* mutants (Figure 2A and Figure S7). We also ensured that all mutants pump at wild-type levels prior to heat shock (Figure 2A). The estimates of ϕ for *hsp-16.41:lin-3c* and *affl-1(sy1202)*; *hsp-16.41:lin-3c* were near zero, which indicates that *affl-1* mutants have no defects in heat-shock-induced *hsp-16.41* expression. The estimates of ϕ for wild type, *Phsp-16.41:lin-3c*; *affl-2(sy975)*, *Phsp-16.41:lin-3c*; *hsf-1(sy441)*, *Phsp-16.41:lin-3c*; *hsf-1(sy1198)*, *Phsp-16.41: affl-2(sy975) affl-1(sy1220)* were all close to one, which indicates that these mutants are not properly expressing the *lin*-3c transgene after heat shock. These results confirmed that *hsf-1* and *affl-2*, but not *affl-1*, are necessary for expression of *hsp-16.41* driven transgenes.

As mentioned above, we noticed that some *affl-2* adults have herniated intestines. We quantified the penetrance of this phenotype in first day adult *hsf-1*, *affl-2*, *affl-1*, and *affl-2 affl-1* double mutants (Figure 2C and Figure S8). We did not observe any herniated adults in N2, *affl-1(sy1202)*, *hsf-1(sy1198)*, and *hsf-1(sy441)* adults. We estimated the frequency of herniated intestines in *affl-2(sy975)* *affl-1(sy1220)* and *affl-2(sy975)* worms to be $0.114^{0.206}_{0.061}$ and $0.113^{0.187}_{0.067}$, respectively (estimated frequency with lower and upper subscripts denoting lower and upper bounds for estimated 95% credible interval). Thus, knocking out *affl-1* does not significantly affect the penetrance of the herniated phenotype in *affl-2* mutants.

affl-2 mutants are deficient in heat-shock-induced gene expression

To examine the role of *affl-2* in heat-shock-induced gene expression, we performed an RNA-seq analysis on *affl-2(sy975)* mutants and wild-type worms with and without heat shock. We performed differential expression analysis and found that the magnitude of transcriptome-wide change in response to heat-shock was reduced in *affl-2* mutants (Figure 3B), and the number of transcripts with a q-value of <0.1 decreased from 3041 to 2277 (Figure 3, C and D). Principal component analysis (PCA) supported the transcriptome shift upon heat shock, dominated by PC1, was reduced in the mutant strain (Figure 3A).

The *hsp-16* and *hsp-70* genes are known to play critical roles in heat shock response, and they have been shown through RNA-seq to be upregulated upon heat shock in an HSF-1 dependent manner (Brunquell *et al.* 2016). Levels of the *hsp-16* and *hsp-70* genes were similar prior to heat shock, but their upregulation upon heat shock was greatly reduced in *affl-2* mutants (Figure 3E). Our RNA-seq results is consistent with the report by Hajdu-Cronin *et al.* (2004), who showed *affl-2* mutants are deficient in heat-shock-induced *hsp-16.2* expression using qPCR. We are thus confident that *affl-2* is a regulator of heat-shock-induced gene expression.

We also fit a linear model on our combined *affl-2(sy975)* and wild-type datasets that included terms to model the

Table 1 DNA Sequence Changes of Alleles

Allele	Sequence change with 25 base pair flanking sequence around the mutation (bold letter)	Predicted amino acid change
hsf-1(sy1198)	GACGACGACAAGCTTCCAGTATTTC **A**GATAAAATTGTGGAATATCGTAGAA	L93Q
affl-2(sy978)	GAAGCTCATTGAGCTTGCGAAGACC **T**GAGGGAAGCTGACGGATGTTGTGGA	R247*
affl-2(sy981)	GTATTTTTTGTACTTGAAGCCATCT **A**GAAAGCTGACAAGGAGCGGACAACT	W456*
affl-2(sy975)	TATTTTTTGTACTTGAAGCCATCTG **A**AAAGCTGACAAGGAGCGGACAACTC	W456*
affl-2(sy509)	AGTGGCTCACGGGACCCCCAAACCA **A**CC**CAC**GTCCGCCGGATCGACACCATCTGGT	Missense mutations starting at S581 R635* and from to frameshift caused by CC to CAC mutation.
affl-2(sy439)	ttttaaaaattgatgaataatttca **A**GTCGCCGTGTTTCAAGGTGTCCGC	Altered splice acceptor site before G482

Alleles *sy439* and *sy509* were both identified in Hajdu-Cronin *et al.* (2004), where *affl-2* was named *sup-45*. All other alleles were identified in this screen. Bold letters indicate modified bp(s) in that allele. Uppercase represents exons and lowercase represents introns

effects of batch, heat shock, genotype, and the interaction between heat shock and genotype. We found that there was significant antagonistic relationship (correlation of $r = -0.71$) between the interaction term and the heat shock term, which supports that the *affl-2* mutant condition diminishes the magnitude of change of many genes upon heat shock (Figure 3F). These results indicate that heat shock response is diminished in *affl-2* mutants and supports our hypothesis that *affl-2* regulates heat-shock-induced transcription.

AFFL-1 and AFFL-2 are homologs of members of the AF4/FMR2 family

Using Jackhmmer (Potter *et al.* 2018), we found that Y55B1BR.2 and Y55B1BR.1 (the paralog of Y55B1BR.2) are homologs of AFF4, which is a member of the AF4/FMR2 family. Based on this homology we chose to name Y55B1BR.1 as *affl-1* (AF4/FMR2 Like) and Y55B1BR.2 as *affl-2*. The AF4/FMR2 family includes the proteins AFF4 and AFF1, which serve as scaffold proteins for multi-subunit super elongation complexes (SECs) that assist with releasing RNA polymerase from promoter-proximal pausing (He and Zhou 2011; Lu *et al.* 2014; Mück *et al.* 2016).

Multiple sequence alignment of *Homo sapiens* AFF1and AFF4 along with *C. elegans* AFFL-2 and AFFL-1 reveals that most of the similarity between the four proteins is in the conserved C-terminal homology domain (CHD) of the AF4/FMR2 family members (Figure 4).The CHD of AFF4 has been shown to bind nucleic acids, form homodimers, and form heterodimers with the AFF1-CHD *in vitro* (Chen and Cramer 2019). Interestingly, our sequence searches identified previously unknown homologs of AF4/FMR2 proteins in *Arabidopsis thaliana*, *Dictyostelium discoideum*, *Acanthamoeba castellani*, and sporadic yeast species (Figure 4B). Gopalan and colleagues previously identified a homolog within *Schizosaccharomyces pombe* (Gopalan *et al.* 2018).

As mentioned above, the clearest similarity of AFFL-2 with AF4 family proteins lies within the CHD. However, important interactions are mediated by the large disordered region toward the N-terminus of the AF4 proteins. AFFL-2 is also predicted to have a disordered N-terminus (Figure S3). Disordered proteins sometimes have protein-binding domains that are disordered in isolation but become structured upon binding (Dosztányi *et al.* 2009), and AFFL-2 has three such predicted disordered protein binding regions in its N-terminus (Figure S3C). An important question is whether the interactions mediated by the AF4 disordered region are conserved in AFFL-2. Addressing this question is challenging computationally for three reasons: (i) binding motifs found within disordered regions tend to be very short, and, thus, difficult to detect with sequence similarity methods; (ii) these motifs are not well conserved at the sequences level; (iii) aligning regions of disordered sequence is inaccurate. With these points in mind, we have annotated the interaction sites in human AFF4 and AFF1 that are known to residue level resolution from resolved protein structures (Figure 4B). These are for P-TEFb binding to AFF4 (Schulze-Gahmen *et al.* 2013), for ELL2 binding to AFF4 (Qi *et al.* 2017), and AF9 binding to AFF1 (Leach *et al.* 2013). Despite the three caveats mentioned above, we can see similarity between AFFL-2, AFF1, and AFF4 at each of the three known binding sites. For each of these interactions to be conserved in *C. elegans*, we would expect the interacting protein to also be found. Through sequence and literature search we identified the *cit-1.1* and *cit-1.2* (Shim *et al.* 2002), *ell-1* (Cai *et al.* 2011), and Y105E8B.7 genes as the *C. elegans* homologs of Cyclin T1, ELL2 and AF9, respectively. In addition to this computational evidence, the interaction of AFFL-2 with the *C. elegans* AF9 homolog was identified in a large-scale interaction screen in *C. elegans* (Simonis *et al.* 2009).

AFFL-2 is a broadly expressed nuclear protein

We cloned the first 3 kb of sequence upstream from the *affl-2* start codon as the promotor of *affl-2*. We used this sequence to create a cGAL driver (Wang *et al.* 2017), which we crossed with a GFP::H2B effector to create a transcriptional reporter for *affl-2*. GFP was visible in all tissues in worms of all stages, which indicates that *affl-2* is ubiquitously expressed (Figure 5A). To observe the subcellular localization of AFFL-2, we created a translational reporter using the cloned the *affl-2* promoter to

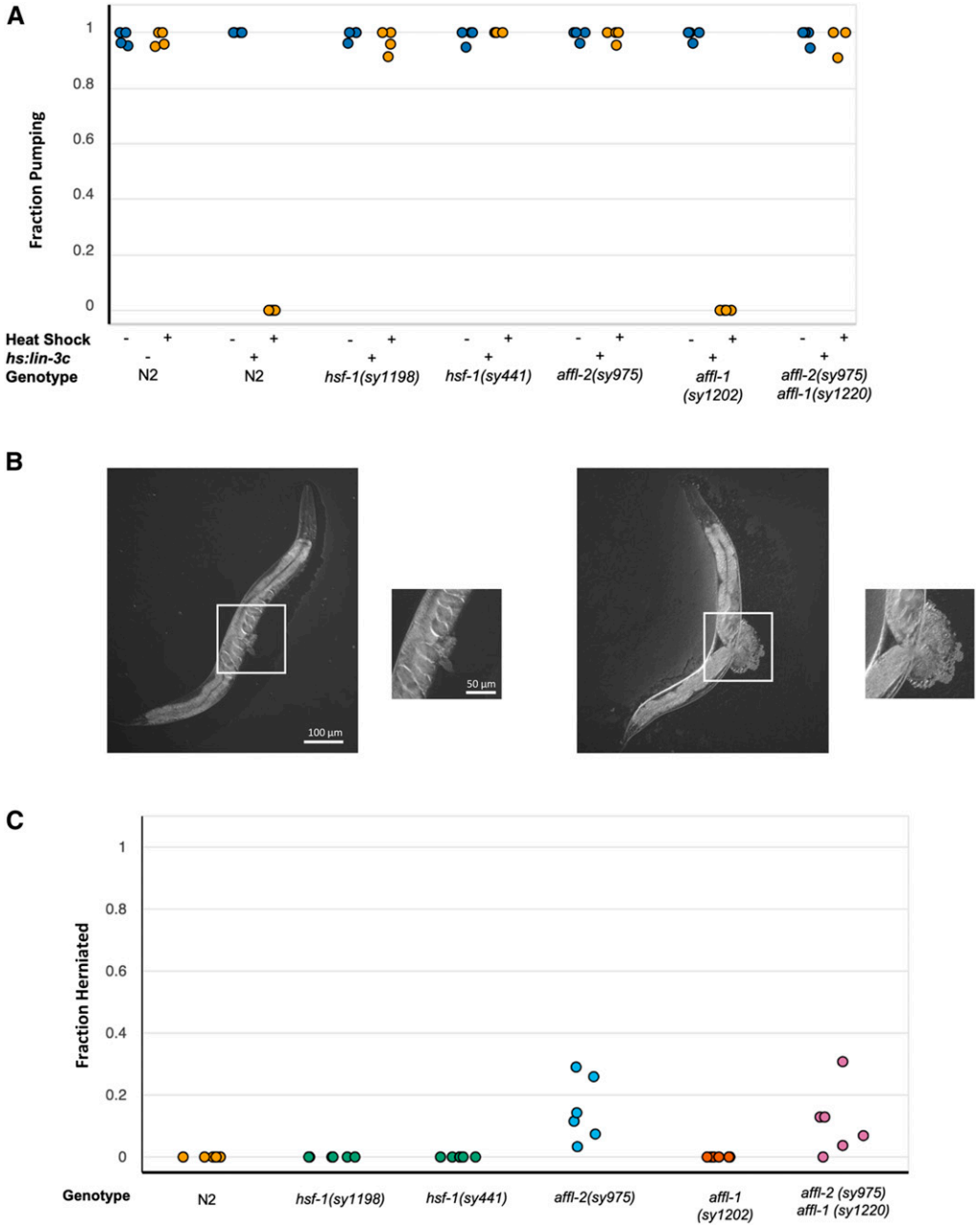

Figure 2 *affl-2* mutants have herniated intestines and are deficient in heat-shock-induced transgene expression. (A) Fraction of worms pumping before and after heat shock to induce P*hsp-16.41: lin-3c* expression. In the *x*-axis *hs: lin-3c* is an abbreviation for the P*hsp-16.41: lin-3c* transgene. Data are a proxy for gene expression (pumping quiescence indicates *hsp-16.41* expression). Each point represents a different trial. (B) Examples of herniated intestines in *affl-2(sy975)* adult animals. (C) Fraction of adult animals with herniated intestines for each genotype. Each point represents a single trial. Data for Figures (A) and (C) can be found at https://doi.org/10.22002/d1.1302.

drive *affl-2 cDNA*::*gfp*. *affl-2(sy975)* mutants with this translational reporter appear wild type and show normal *lin-3c*-induced pumping quiescence after heat shock (Figure 5, E and F). Therefore, we believe that our fusion protein is functional, and our cloned promoter for *affl-2* reflects its endogenous expression pattern. We found that AFFL-2 is predicted to have two NLSs, which suggested that it is a nuclear protein (Figure 1D, see *Materials and Methods*). Indeed, AFFL-2::GFP is exclusively located in the nucleus prior to heat shock, and we do not see any noticeable difference in AFFL-2::GFP localization or intensity between worms before and after heat shock (Figure 5B).

As shown above, *affl-1* is not necessary for heat-shock-induced *hsp-16.41* transcription, despite encoding a homolog of AFF1 and AFF4. Our multiple sequence alignment suggests that AFFL-1 shares little similarity with the first 135 amino acids of AFFL-2, and AFFL-1 is not predicted to have an NLS (Figure 4, see *Materials and Methods*). We thus decided to investigate the role of the N-terminus of AFFL-2, which contains its predicted NLSs and the majority of its predicted disordered residues (Figure 1D and Figure S3C) by creating AFFL-2 variants with modified N termini (Figure 5C). First, we created a modified AFFL-2::GFP in which we removed 129 amino acids from the N terminus of AFFL-2. This modification eliminated both predicted NLSs and the majority of the disordered residues. To test the necessity of the disordered residues independently from the NLS, we created a

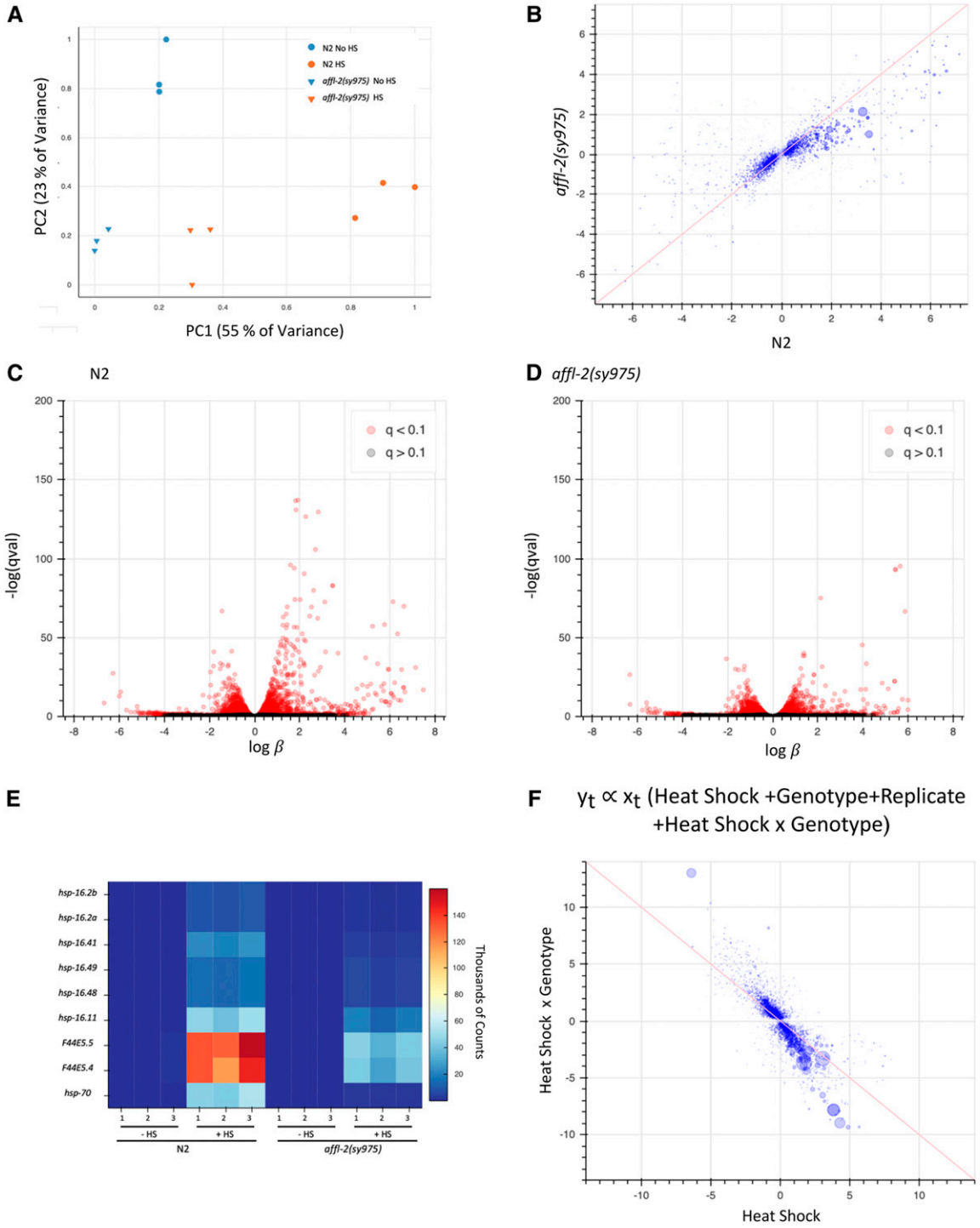

Figure 3 *affl-2(sy975)* mutants have a compromised transcriptional response to heat shock. (A) Principal component analysis (PCA) of estimated transcript counts data in RNA-seq samples. (B) Comparison of β s, proportional to the log fold-change, due to heat shock treatment for N2 and *affl-2(sy975)* mutants. β is a biased estimator of the fold change due to heat shock treatment. Pearson correlation of plotted data are $r = 0.40$. Volcano plots for effect of heat shock on N2 (C) and *affl-2 (sy975)* (D). (E) Heat map of estimated transcript counts for *hsp-16* and *hsp-70* genes. (F) Comparison of β s corresponding to heat shock treatment and to interaction between heat shock and genotype. Pearson correlation of plotted data are $r = -0.71$. In scatter plots (B) and (F), pink line is at $x = y$ and x = -y respectively, and size of points is proportional to the $-\log(\text{qval})$ of a given gene.

construct in which we substituted the deleted residues with the SV40 NLS. To test the role of the disordered nature of the domain independently of its sequence, we made another construct that included the artificial NLS and the 212-residue fused in sarcoma low complexity (FUS LC) domain. FUS is one of three RNA binding proteins with low-complexity domains that, when fused to DNA-binding domains, cause a variety of cancers (Arvand and Denny 2001; Guipaud *et al.*

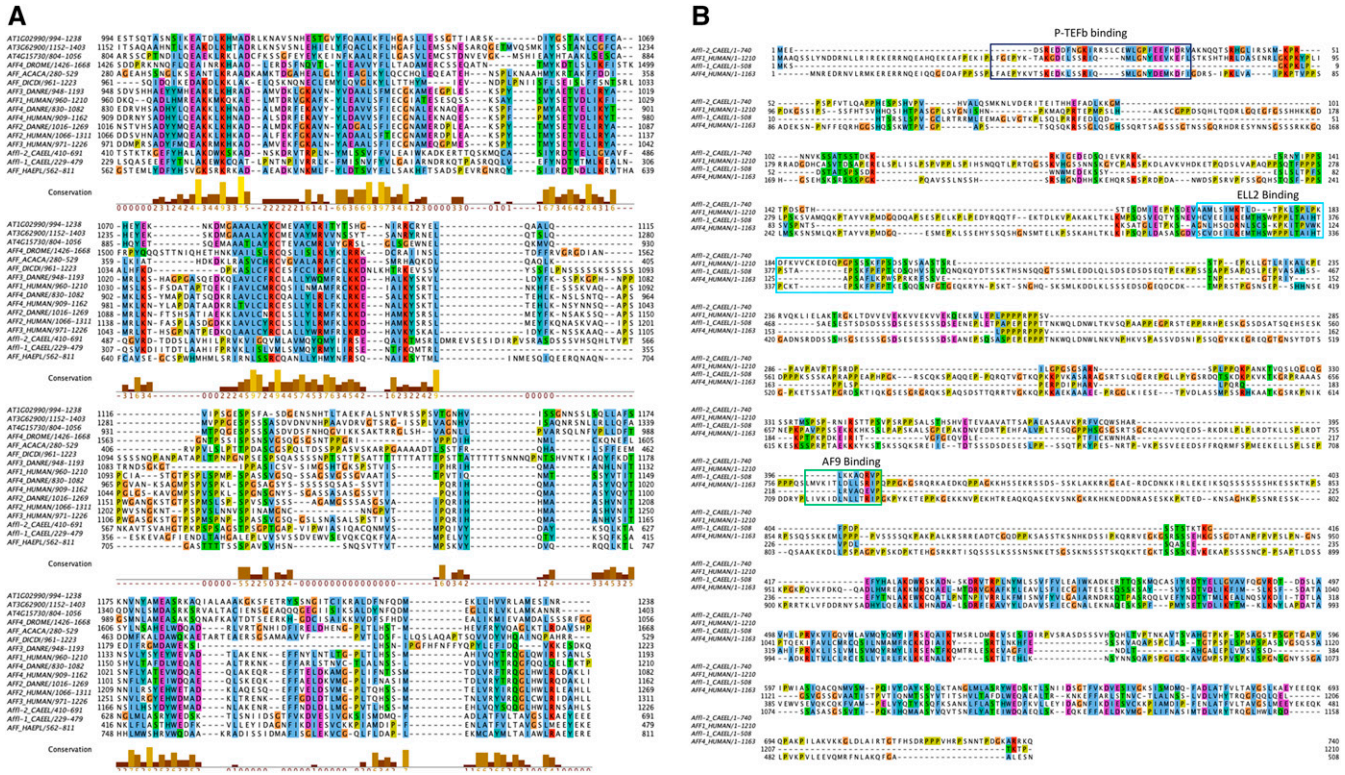

Figure 4 AF4/FMR2 family members are widely conserved. (A) Alignment of example AF4/FMR2 C-terminal homology domains generated by MUSCLE software. (B) Sequence alignment of AFFL-2, AFFL-1 (AFFL-2 paralog in *C. elegans*), and AFF1 and AFF4 in *H. sapiens*. AFF4 binding sties for AF9, ELL2, P-TEFb are annotated (Chou *et al.* 2013; Leach *et al.* 2013; Schulze-Gahmen *et al.* 2013; Qi *et al.* 2017; Schulze-Gahmen and Hurley 2018; Chen and Cramer 2019). Both alignments are rendered using the Jalview package with ClustalX color scheme. Conserved residues are colored as follows: hydrophobic (blue), positive charge (red), negative charge (magenta), polar (green), cysteines (pink), glycine (orange), proline (yellow) and aromatic (cyan). The UniProtKB accession identifiers for each sequence in (A) are listed here: At1g02990, F4HZA0; At3g62900, F4IZK5; At4g15730, Q8GY51; AFF4_DROME, Q9VQI9; AFF_ACACA, L8H858; AFF_DICDI, Q54 PM 6; AFF3_DANRE, F1RA06; AFF1_HUMAN, P51825; AFF4_DANRE, I3ISK1; AFF4_HUMAN, Q9UHB7; AFF2_DANRE, E7F2E1; AFF2_HUMAN, P51816; AFF3_HUMAN, P51826; AFFL-2_CAEEL, Q95XW7; AFFL-1_CAEEL, Q95XW6; AFF_HAEPL, A0A158QQA2. The UniProtKB accession identifiers for each sequence in (B) are listed here: AFFL-2_CAEEL, Q95XW7; AFFL-1_CAEEL, Q95XW6; AFF1_HUMAN, P51825; AFF4_HUMAN, Q9UHB7.

2006; Lessnick and Ladanyi 2012); 84% of the FUS LC domain consists of glycine, serine, glutamine, and tyrosine, and, at high concentrations, the domain has been shown to polymerize. Kwon *et al.* (2013) also demonstrated that the FUS LC domain fused to the GAL4 DNA binding domain can induce transcriptional activation. As a control, we added a similar region but with 10 tyrosines mutated to serines, as this modification was shown to prevent the GAL4 and FUS LC fusion transcriptional activation abilities (Kwon *et al.* 2013).

We found that, in a wild-type background, all of the altered AFFL-2 proteins containing an NLS are observed in the nucleus (Figure 5D). The modified AFFL-2 lacking the artificial NLS is located primarily in the nucleus, but we saw that some of the protein is present in the cytoplasm (Figure 5D and Figure S4). To test whether the nuclear localization of this construct is dependent on the presence of wild-type AFFL-2, we introduced the modified AFFL-2 with N-terminal deletion in *affl-2(sy975)* animals. The localization of AFFL-2::N-terminal deletion::GFP was similar in both a wild-type and *affl-2(sy975)* background: some animals had it strictly localized to the nucleus, whereas others had it in the cytoplasm as well (Figure S4). We did not expect this modified protein to localize to the nucleus, but this result suggests there is an alternative mechanism for its nuclear import.

We examined the extent to which each construct rescued the herniated intestine phenotype through quantifying the fraction of herniated adults in each genotype. Note that all but N2 worms had a P*hsp-16.41: lin-3c* transgene in their background. We did not observe any herniated intestines in *affl-2(sy975)* adults with either the full rescue construct, the artificial NLS only construct, or the FUS LC and artificial NLS construct (Figure 5F). On the other hand, we observed herniated intestines in *affl-2(sy975)* mutants with the deletion-only construct with similar frequency to *affl-2(sy975)* mutants (Figure 5F and Figure S8). The frequency of hernias in *affl-2(sy975)* adults with the modified (tyrosine to serine) FUS LC domain was nonzero but less than that of *affl-2(sy975)* mutants without any rescue construct (Figure 5F and Figure S8). Additionally, we noticed that *affl-2(sy975)* mutants with the full construct consistently appeared wild type, whereas *affl-2(sy975)* with the other constructs qualitatively looked more like *affl-2(sy975)* mutants (Figure S5).

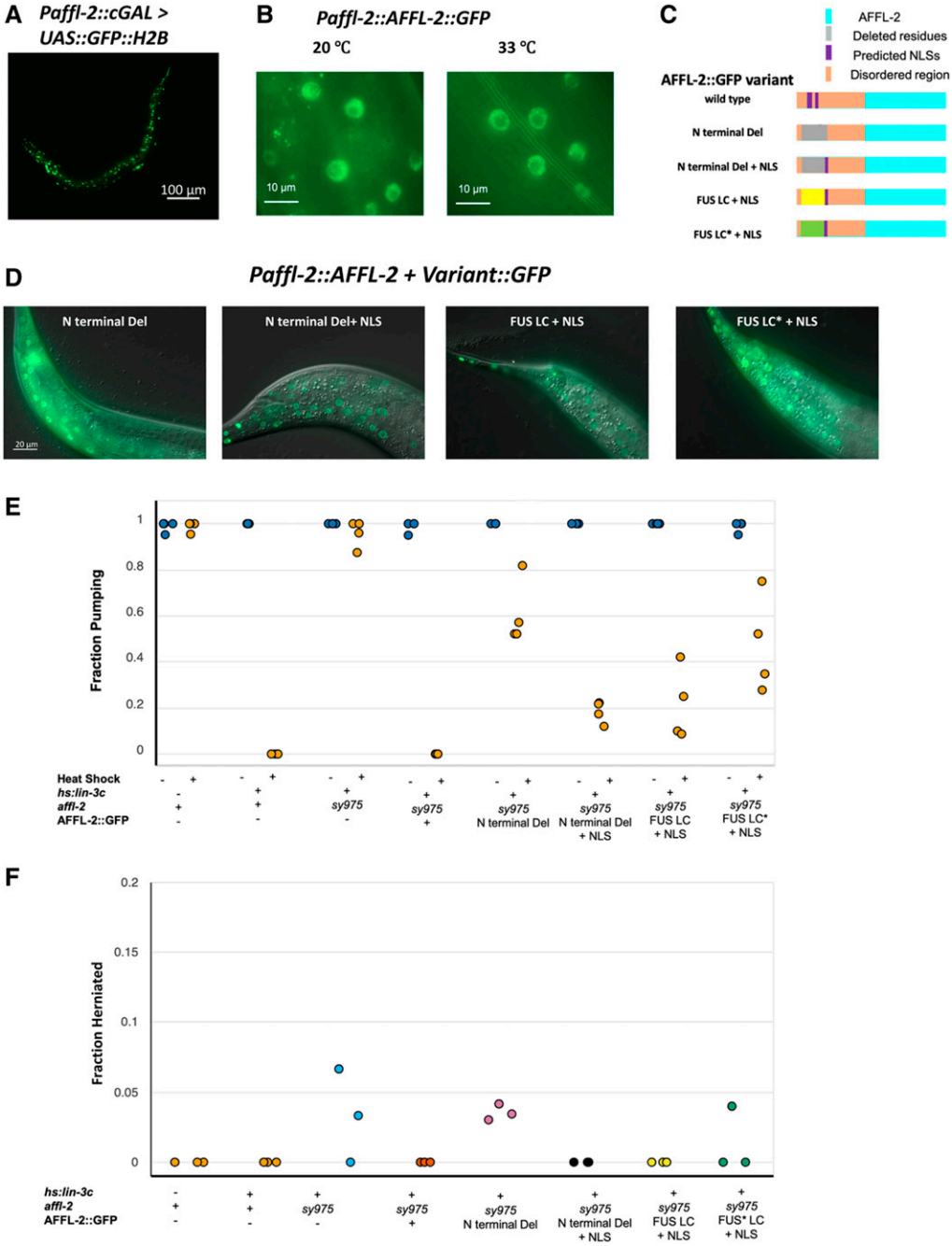

Figure 5 AFFL-2 is a ubiquitously expressed nuclear protein. (A) Representative image of a worm expressing *Paffl-2*::*cGAL* > *15xUAS*::*GFP*::*H2B*, which can be seen in the majority of cells, indicating that *affl-2* is ubiquitously expressed. Note that the effector construct is integrated, while the driver is an extrachromosomal array. (B) AFFL-2::GFP at 20° and 33°. Both images are taken of nuclei in the tail of young adults and are representative of the AFFL-2::GFP localization throughout the body. (C) Diagrams of AFFL-2 variants. Note that diagrams are not to scale and are just representative of the ordering of various elements. FUS LC* represents the modified FUS LC residues with disordered residues mutated to more ordered ones. All constructs are driven by the *affl-2* promoter (P*affl-2*). (D) Subcellular of localization of AFFL-2 variants. Animals in photos are young wild type adults at 20°. (E) Fraction of worms pumping before or after heat shock to induce P*hsp-16.41: lin-3c* expression. Note that *hs:lin-3c* is an abbreviation for the P*hsp-16.41: lin-3c* transgene. Data are a proxy for gene expression (pumping quiescence indicates *hsp-16.41* expression). Each point represents a different trial. (F) Fraction of adult worms with herniated intestines. Each point represents a different trial. Data for Figures (E) and (F) can be found at https://doi.org/10.22002/d1.1302.

To determine the extent that the constructs rescued the heat-shock-induced gene expression defects of *affl-2(sy975)*, we estimated the probability of worms exhibiting pumping quiescence due to heat-shock-induced *Phsp-16.41: lin-3c* expression (Figure 5E and Figure S7). The estimate of ϕ (the probability of pumping after heat shock) for *affl-2(sy975)* animals with a wild type copy of AFFL-2::GFP was near zero, which demonstrates that the full AFFL-2::GFP construct is functional. The estimates for ϕ for the deletion-only construct and the construct with the addition of the modified FUS LC domain were both relatively high ($0.607^{0.720}_{0.470}$, $0.485^{0.629}_{0.336}$), and the estimates for ϕ for constructs with only the artificial NLS and the FUS LC were much lower ($0.190^{0.293}_{0.111}$ and $0.210^{0.352}_{0.119}$, respectively).

Even though the modified AFFL-2 with both predicted NLSs removed can be seen in the nucleus, adding back the artificial NLS significantly increased the performance of AFFL-2, as seen in both our herniated intestine and quiescence experiments. This observation suggests that exclusive restriction of AFFL-2 in the nucleus is important for its function. Adding back the low complexity FUS LC did not further increase the performance of the modified AFFL-2, but the

modified (tyrosine to serine) FUS LC hindered the performance of AFFL-2.

affl-1 and affl-2 do not significantly influence HSF-1 localization and expression

We used an *hsf-1* translational reporter to determine if *affl-2* and/or *affl-1* are necessary for proper localization and expression of HSF-1. *C. elegans* HSF-1 is a ubiquitously expressed nuclear protein, and HSF-1 will aggregate to form nuclear stress granules after heat shock (Morton and Lamitina 2013). The HSF-1 foci do align with marks of active transcription, and are dependent on the HSF1 DNA-binding domain, but the putative sites of the foci are still unknown (Morton and Lamitina 2013). We quantified the formation of granules after heat shock using the *Phsf-1*::HSF-1::GFP transgene from Morton and Lamitina (2013). We also quantified the intensity of the granules after heat shock and the intensity of HSF1::GFP prior to heat shock for all genotypes (Figure S6). We found that HSF-1 expression prior to heat shock is similar in all genotypes (Figure S6A), which suggests that neither *affl-2* nor *affl-1* are critical for regulating HSF1 expression. Although there are differences in the median number of granules and intensity of HSF-1::GFP between genotypes, there is too much overlap between the distributions of granule intensity and number for these differences to fully explain the highly nonoverlapping differences between the morphological and P*hsp-16.41*::*lin-3c* overexpression quiescence phenotype of different strains (Figure 6B and Figure S6). *affl-1(sy1202)* worms (estimated median of eight granules/nucleus) have more granules per nucleus compared to wild type worms (estimated median seven granules/nucleus). *affl-2* (*sy975)* mutants and *affl-2(sy975) affl-1(sy1220)* formed slightly fewer granules after heat shock (estimated median six granules/nucleus). These results do not explain why *affl-2(sy975)* worms are unable to express *hsp-16.41*, as some wild type worms had similar HSF-1 granule numbers per nuclei and similar HSF-1::GFP levels. Since HSF-1 localization and expression is not significantly disrupted in *affl-2* mutants, we believe that AFFL-2 acts either downstream of, or parallel to, HSF-1 to regulate heat-shock-induced transcription in *C. elegans*.

Discussion

We have cloned and performed a genetic analysis of *affl-2*—a homolog of AF4/FMR2 family members—and shown that *affl-2* regulates heat-shock-induced transcription. Through a forward genetic screen for suppressors of heat-shock-induced *lin-3c* overexpression, we identified one new *hsf-1* allele and three *affl-2* alleles. To our knowledge, this is the first isolated viable *hsf-1* allele with an altered DNA-binding domain. Our RNA-seq analysis of *affl-2* mutants and wild-type animals demonstrates that *affl-2* mutants are deficient in the heat-shock-induced transcriptional changes normally found in wild-type animals. We also found that *affl-2* mutants have herniated intestines, whereas animals lacking a functional *affl-1*—another homolog of AF4/FMR2 family members and the paralog of *affl-2*— appear wild type. We determined that *affl-2* is a ubiquitously expressed nuclear protein, and proper localization is necessary for its role in heat-shock-induced gene expression. Finally, we showed that *affl-2* is not necessary for formation of heat-shock-induced HSF-1 nuclear granules.

affl-2 mutants had been identified in another screen for suppressors of heat-shock-induced gene expression, and that screen also identified *hsf-1* and *cyl-1* as regulators of heat-shock response (Hajdu-Cronin *et al.* 2004). Taken together, these two studies illustrate the power of simple genetic screens in *C. elegans* to find regulators of gene expression. We did not recover any *cyl-1* mutants, but data from Hajdu-Cronin *et al.* (2004) suggests that *cyl-1* may not be necessary for heat-shock-induced *hsp-16.41* transcription. We did not perform further study of *cyl-1*, but it is possible that it regulates only a subset of heat-shock-induced transcription.

Brunquell *et al.* (2016) demonstrated through RNA-seq that heat-shock-induced upregulation of the *hsp-16* and *hsp-70* genes is dependent on HSF-1. We conducted a similar experiment to Brunquell *et al.* (2016) to profile the transcriptome of *affl-2(sy975)* mutants before and after heat shock, and we found that heat-shock-dependent induction of the *hsp-16* and *hsp-70* genes is impaired in *affl-2* mutants. We also found that the global heat-shock-induced transcriptional phenotype is impaired in *affl-2* mutants, which indicates that *affl-2* is necessary for heat-shock-induced transcription. Thus, like *hsf-1*, *affl-2* is a key component of heat-shock-induced gene expression.

Along with conservation in the CHD, we see weak conservation of AFF4's AF9/ENL, ELL-1/2, and P-TEFb binding sites in the AFFL-2 N terminal sequence (Figure 4B). AFFL-2 is predicted computationally to have three candidates for binding sites, but we have not yet tested whether these are used. Our deletion removed the region of AFFL-2 similar to AFF4's binding site to P-TEFb, and, thus, we expected it to be necessary for AFFL-2 function. Surprisingly, we found that replacing much of the disordered N-terminus of AFFL-2 with an exogenous NLS restores protein function to ~80% of the wild-type control, even though the modified AFFL-2 with its predicted NLSs at the N-terminus removed still partially localizes to the nucleus. It is possible that the C-terminus of AFFL-2 may contain a weak NLS that cannot be predicted by current software that allows AFFL-2 to partially localize to the nucleus at low levels. Addition of an exogenous NLS could be necessary to increase the concentration of nuclear AFFL-2 to improve its functioning but does not restore AFFL-2 activity to wild-type levels. Adding a disordered domain, the FUS LC domain, does not further restore AFFL-2 activity. It is believed that FUS increases transcriptional activity by enhancing recruitment of RNA polymerase II, for mutants that bind RNA polymerase II better increase transcription (Kwon *et al.* 2013), and thus this result suggests that the role of AFFL-2 is not to enhance recruitment of RNA polymerase. The residues we deleted remove only one of the candidate

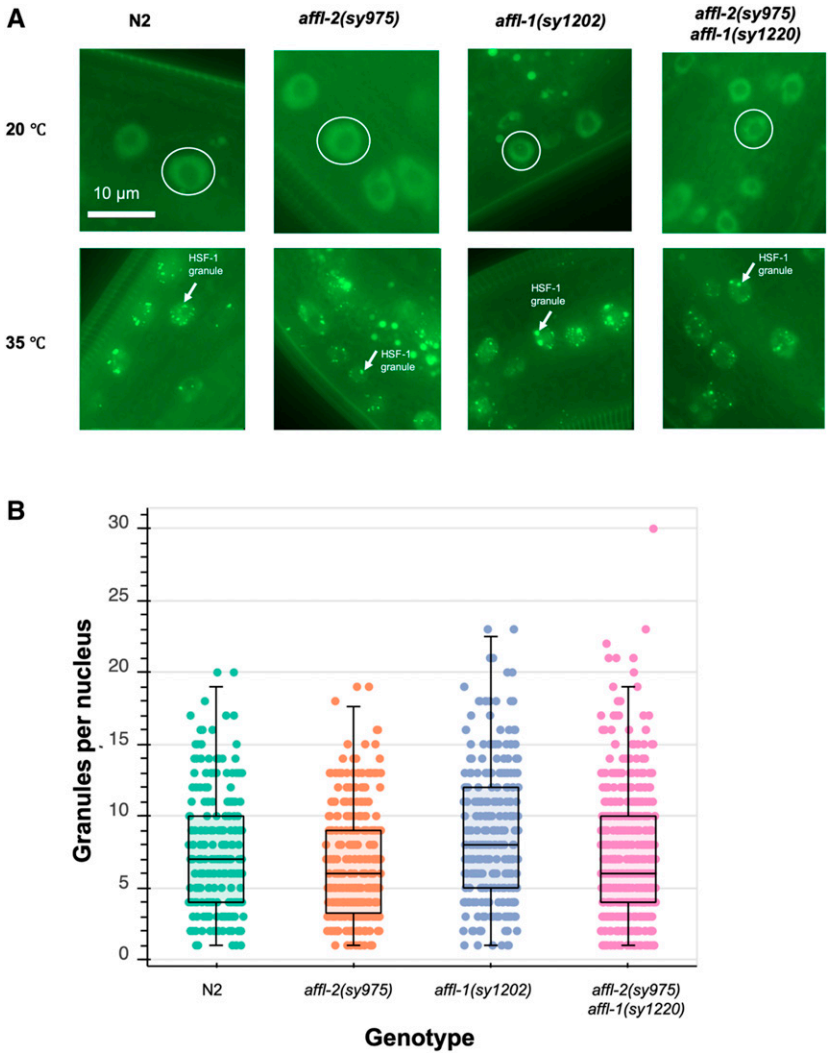

Figure 6 Analysis of the interaction of *hsf-1*, *affl-2*, and *affl-1*. All genotypes contain *drSi13*, which is the single-copy transgene with P*hsf-1*::HSF-1::GFP. (A) Representative images of hypodermis nuclei in young adults. Subcellular localization of HSF-1::GFP with and without a 5-min heat shock at 35°. Prior to heat shock, HSF-1::GFP is distributed throughout the nucleus for all genotypes; after heat shock HSF-1::GFP forms nuclear granules. Images of nuclei are from the hypodermis but are representative of HSF-1::GFP localization throughout the entire animal. In top row, representative nuclei are circled. In bottom row, examples of nuclear granules are indicated with arrows. (B) Quantification of HSF-1::GFP granules per nucleus after heat shock for different genotypes. Each point represents one nucleus. Box plots represent the 25th percentile (bottom of box), median (center line of box), and 75th percentile (top of box) of the data. Data are from 15 N2, 19 *affl-2(sy975)*, 13 *affl-1(sy1202)*, and 21 *affl-2(sy975) affl-1(sy1220)* animals.

binding sites of AFFL-2, and it is possible that the other binding sites and disordered residues can act redundantly to maintain AFFL-2 activity. However, a more thorough biochemical investigation of AFFL-2 is needed to determine the role of different domains of the protein.

Despite AFFL-1 being homologous to AFF4/AFF1, AFFL-1 is not necessary for heat-shock-induced expression of the P-*hsp-16.41*::*lin-3c* transgene, and *affl-1* mutants appear wild type. AFFL-1 is not predicted to have any nuclear localization signals, but since we do not have a phenotype for *affl-1* mutants, we cannot validate any expression pattern or localization obtained using a fusion construct. We have not fully investigated *affl-1* mutants to see if they have any deficiencies in other processes, or whether *affl-1* plays a redundant role with another gene.

We used translational reporters to examine the roles of *affl-1* and *affl-2* on HSF-1 subcellular localization and expression. While we did find some differences in HSF-1 expression prior to heat shock and HSF-1 granule formation after heat shock, we do not believe that these differences can explain the phenotypes of the various mutants due to the high overlap between the distributions of our measurements for different genotypes. Thus, we believe that AFFL-2 does not regulate HSF-1 granule formation, which suggests that AFFL-2 acts downstream or parallel to granule formation. We hypothesize that AFFL-2 acts downstream of granule formation, for AFFL-2 is homologous to regulators of elongation. The sequences required for interaction with the granules are not known, and it is still unclear what their role in heat shock response is (Morton and Lamitina 2013). It is possible that these granules are representative of a process that acts parallel to AFFL-2 regulated heat-shock-induced transcription.

As mentioned previously, AFFL-1 and AFFL-2 are homologs of mammalian AFF1 and AFF4. AFF1 and AFF4 serve as scaffolds in the super elongation complex (SEC), which regulates release from promoter-proximal pausing during transcriptional elongation using P-TEFb (He and Zhou 2011; Lu *et al.* 2014; Mück *et al.* 2016). Like AFFL-2, AFF4 regulates heat-shock-induced HSP70 expression, which illustrates that its role in heat-shock-induced gene expression is conserved

(Lu *et al.* 2015). In *C. elegans*, the P-TEFb complex has been shown to be necessary for embryonic development and expression of *hsp-16.2* (Schulze-Gahmen *et al.* 2013). The *C. elegans* homolog of the ELL gene family (*ell-1*) and its partner (*eaf-1)* are necessary for embryonic development and heat-shock-induced transcription (Cai *et al.* 2011). If the role of AFFL-2 was restricted to heat-shock-induced gene expression, we would expect *affl-2* mutants to appear wild type outside of heat-shock response. However, we have observed and quantified the presence of hernias in *affl-2* mutants, which suggests that *affl-2* may regulate other processes. Furthermore, Hajdu-Cronin *et al.* (2004) reported that *affl-2* mutants are Dpy and Egl. *hsf-1* is known to play a role in development and aging in addition to heat-shock response (Hajdu-Cronin *et al.* 2004; Li *et al.* 2016). Future work should investigate whether *affl-2* plays a role in development, and, if so, compare this role to that of *hsf-1* and other SEC homologs in *C. elegans*.

Our results demonstrate that the *C. elegans* ortholog of AF4/FMR2 family members, AFFL-2, is necessary for heat-shock-induced transcription. Our sequence analysis suggests that AF4/FMR2 homologs are found more widely in nature than previously thought, highlighting their importance. It would thus be worthwhile to see if AF4/FMR2 homologs in other systems also regulate heat-shock response to see if this function is conserved. These results combined with previous work on other members of the SEC suggest that *C. elegans* can be a powerful, multicellular model to understand transcription. We believe that further study of *C. elegans* homologs of human AF4/FMR2 proteins will facilitate our understanding of heat-shock response.

Acknowledgments

We thank Heenam Park for helping create putative *affl-1* null mutants using CRISPR/Cas9, and Jean Badroos, Jasmine S. Revanna, and Minyi Tan for technical assistance. We thank Hillel Schwartz, Jonathan Liu, and members of the Sternberg laboratory for insightful discussions. We thank Sarah MacLean and the Sternberg laboratory members for comments on the manuscript. Some strains were provided by the Caenorhabditis Genetics Center (CGC), which is funded by the National Institutes of Science (NIH) Office of Research Infrastructure Programs (P40 OD010440). This work was supported by National Institutes of Heath grant (K99GM126137 to H.W., U24HG002223 to P.W.S., and R240D023041). The Millard and Muriel Jacobs Genetics and Genomics Laboratory at California Institute of Technology performed whole genome sequencing and RNA-sequencing. S.J.W. was supported by the Caltech Student Faculty Programs, the family of Laurence J. Stuppy, Samuel N. Vodopia, and Carol J. Hasson.

Literature Cited

Åkerfelt, M., R. I. Morimoto, and L. Sistonen, 2010 Heat shock factors: integrators of cell stress, development and lifespan. Nat. Rev. Mol. Cell Biol. 11: 545–555. https://doi.org/10.1038/nrm2938

Arvand, A., and C. T. Denny, 2001 Biology of EWS/ETS fusions in Ewing's family tumors. Oncogene 20: 5747–5754. https://doi.org/10.1038/sj.onc.1204598

Baugh, L. R., J. DeModena, and P. W. Sternberg, 2009 RNA Pol II accumulates at promoters of growth genes during developmental arrest. Science 324: 92–94. https://doi.org/10.1126/science.1169628

Bois J., 2018 bebi103. https://github.com/justinbois/bebi103

Brameier, M., A. Krings, and R. M. MacCallum, 2007 NucPred–predicting nuclear localization of proteins. Bioinformatics 23: 1159–1160. https://doi.org/10.1093/bioinformatics/btm066

Bray, N. L., H. Pimentel, P. Melsted, and L. Pachter, 2016 Near-optimal probabilistic RNA-seq quantification. Nat. Biotechnol. 34: 525–527 (erratum: Nat. Biotechnol. 34: 888). https://doi.org/10.1038/nbt.3519

Brenner, S., 1974 The genetics of Caenorhabditis elegans. Genetics 77: 71–94.

Brunquell, J., S. Morris, Y. Lu, F. Cheng, and S. D. Westerheide, 2016 The genome-wide role of HSF-1 in the regulation of gene expression in Caenorhabditis elegans. BMC Genomics 17: 559. https://doi.org/10.1186/s12864-016-2837-5

Cai, L., B. L. Phong, A. L. Fisher, and Z. Wang, 2011 Regulation of fertility, survival, and cuticle collagen function by the Caenorhabditis elegans eaf-1 and ell-1 genes. J. Biol. Chem. 286: 35915–35921. https://doi.org/10.1074/jbc.M111.270454

Chen, Y., and P. Cramer, 2019 Structure of the super-elongation complex subunit AFF4 C-terminal homology domain reveals requirements for AFF homo- and heterodimerization. J. Biol. Chem. 294: 10663–10673. https://doi.org/10.1074/jbc.RA119.008577

Chou, S., H. Upton, K. Bao, U. Schulze-Gahmen, A. J. Samelson *et al.*, 2013 HIV-1 Tat recruits transcription elongation factors dispersed along a flexible AFF4 scaffold. Proc. Natl. Acad. Sci. USA 110: E123–E131. https://doi.org/10.1073/pnas.1216971110

Dai, C., L. Whitesell, A. B. Rogers, and S. Lindquist, 2007 Heat shock factor 1 is a powerful multifaceted modifier of carcinogenesis. Cell 130: 1005–1018. https://doi.org/10.1016/j.cell.2007.07.020

Doitsidou, M., R. J. Poole, S. Sarin, H. Bigelow, and O. Hobert, 2010 C. elegans mutant identification with a one-step whole-genome-sequencing and SNP mapping strategy. PLoS One 5: e15435. https://doi.org/10.1371/journal.pone.0015435

Dosztányi, Z., V. Csizmok, P. Tompa, and I. Simon, 2005 IUPred: web server for the prediction of intrinsically unstructured regions of proteins based on estimated energy content. Bioinformatics 21: 3433–3434. https://doi.org/10.1093/bioinformatics/bti541

Dosztányi, Z., B. Mészáros, and I. Simon, 2009 ANCHOR: web server for predicting protein binding regions in disordered proteins. Bioinformatics 25: 2745–2746. https://doi.org/10.1093/bioinformatics/btp518

Dosztányi Z., V. Csizmok, P. Tompa, and I. Simon, 2005 IUPred: web server for the prediction of intrinsically unstructured regions of proteins based on estimated energy content. Bioinformatics 21: 3433–3434. https://doi.org/10.1093/bioinformatics/bti541

Edgar, R. C., 2004 MUSCLE: multiple sequence alignment with high accuracy and high throughput. Nucleic Acids Res. 32: 1792–1797. https://doi.org/10.1093/nar/gkh340

Gopalan, S., D. M. Gibbon, C. A. Banks, Y. Zhang, L. A. Florens *et al.*, 2018 Schizosaccharomyces pombe Pol II transcription elongation factor ELL functions as part of a rudimentary super elongation complex. Nucleic Acids Res. 46: 10095–10105. https://doi.org/10.1093/nar/gky713

Guipaud, O., F. Guillonneau, V. Labas, D. Praseuth, J. Rossier *et al.*, 2006 An in vitro enzymatic assay coupled to proteomics analysis reveals a new DNA processing activity for Ewing sarcoma and TAF(II)68 proteins. Proteomics 6: 5962–5972. https://doi.org/10.1002/pmic.200600259

Hajdu-Cronin, Y. M., W. J. Chen, and P. W. Sternberg, 2004 The L-type cyclin CYL-1 and the heat-shock-factor HSF-1 are required for heat-shock-induced protein expression in Caenorhabditis elegans. Genetics 168: 1937–1949. https://doi.org/10.1534/genetics.104.028423

He, N., and Q. Zhou, 2011 New insights into the control of HIV-1 transcription: when tat meets the 7SK snRNP and super elongation complex (SEC). J. Neuroimmune Pharmacol. 6: 260–268. https://doi.org/10.1007/s11481-011-9267-6

Hsu, A.-L., C. T. Murphy, and C. Kenyon, 2003 Regulation of aging and age-related disease by DAF-16 and heat-shock factor. Science 300: 1142–1145 (erratum: Science 300: 2033). https://doi.org/10.1126/science.1083701

Virtanen, P., R. Gommers, T. E. Oliphant, M. Haberland, T. Reddy *et al.*, 2020 SciPy 1.0: Fundamental Algorithms for Scientific Computing in Python. Nat. Meth. (in press).

Kosugi, S., M. Hasebe, T. Entani, S. Takayama, M. Tomita *et al.*, 2008 Design of peptide inhibitors for the importin alpha/beta nuclear import pathway by activity-based profiling. Chem. Biol. 15: 940–949. https://doi.org/10.1016/j.chembiol.2008.07.019

Kosugi, S., M. Hasebe, N. Matsumura, H. Takashima, E. Miyamoto-Sato *et al.*, 2009a Six classes of nuclear localization signals specific to different binding grooves of importin alpha. J. Biol. Chem. 284: 478–485. https://doi.org/10.1074/jbc.M807017200

Kosugi, S., M. Hasebe, M. Tomita, and H. Yanagawa, 2009b Systematic identification of cell cycle-dependent yeast nucleocytoplasmic shuttling proteins by prediction of composite motifs. Proc. Natl. Acad. Sci. USA 106: 10171–10176. https://doi.org/10.1073/pnas.0900604106

Kuras, L., and K. Struhl, 1999 Binding of TBP to promoters in vivo is stimulated by activators and requires Pol II holoenzyme. Nature 399: 609–613. https://doi.org/10.1038/21239

Kwon, I., M. Kato, S. Xiang, L. Wu, P. Theodoropoulos *et al.*, 2013 Phosphorylation-regulated binding of RNA polymerase II to fibrous polymers of low-complexity domains. Cell 155: 1049–1060 [corrigenda: Cell 156: 374 (2014)]. https://doi.org/10.1016/j.cell.2013.10.033

Leach, B. I., A. Kuntimaddi, C. R. Schmidt, T. Cierpicki, S. A. Johnson *et al.*, 2013 Leukemia fusion target AF9 is an intrinsically disordered transcriptional regulator that recruits multiple partners via coupled folding and binding. Structure 21: 176–183. https://doi.org/10.1016/j.str.2012.11.011

Lenasi, T., and M. Barboric, 2010 P-TEFb stimulates transcription elongation and pre-mRNA splicing through multilateral mechanisms. RNA Biol. 7: 145–150. https://doi.org/10.4161/rna.7.2.11057

Lessnick, S. L., and M. Ladanyi, 2012 Molecular Pathogenesis of Ewing Sarcoma: New Therapeutic and Transcriptional Targets. Annu. Rev. Pathol. Mech. Dis. 7: 145–159. https://doi.org/10.1146/annurev-pathol-011110–130237

Levine, M., 2011 Paused RNA polymerase II as a developmental checkpoint. Cell 145: 502–511. https://doi.org/10.1016/j.cell.2011.04.021

Li, J., L. Chauve, G. Phelps, R. M. Brielmann, and R. I. Morimoto, 2016 E2F coregulates an essential HSF developmental program that is distinct from the heat-shock response. Genes Dev. 30: 2062–2075. https://doi.org/10.1101/gad.283317.116

Li, J., J. Labbadia, and R. I. Morimoto, 2017 Rethinking HSF1 in stress, development, and organismal health. Trends Cell Biol. 27: 895–905. https://doi.org/10.1016/j.tcb.2017.08.002

Lin, C., E. R. Smith, H. Takahashi, K. C. Lai, S. Martin-Brown *et al.*, 2010 AFF4, a component of the ELL/P-TEFb elongation complex and a shared subunit of MLL chimeras, can link transcription elongation to leukemia. Mol. Cell 37: 429–437. https://doi.org/10.1016/j.molcel.2010.01.026

Lin, C., A. S. Garrett, B. D. Kumar, E. R. Smith, M. Gogol *et al.*, 2011 Dynamic transcriptional events in embryonic stem cells mediated by the super elongation complex (SEC). Genes Dev. 25: 1486–1498. https://doi.org/10.1101/gad.2059211

Lu, H., Z. Li, Y. Xue, U. Schulze-Gahmen, J. R. Johnson *et al.*, 2014 AFF1 is a ubiquitous P-TEFb partner to enable Tat extraction of P-TEFb from 7SK snRNP and formation of SECs for HIV transactivation. Proc. Natl. Acad. Sci. USA 111: E15–E24. https://doi.org/10.1073/pnas.1318503111

Lu, H., Z. Li, W. Zhang, U. Schulze-Gahmen, Y. Xue *et al.*, 2015 Gene target specificity of the Super Elongation Complex (SEC) family: how HIV-1 Tat employs selected SEC members to activate viral transcription. Nucleic Acids Res. 43: 5868–5879. https://doi.org/10.1093/nar/gkv541

Luo, Z., C. Lin, E. Guest, A. S. Garrett, N. Mohaghegh *et al.*, 2012a The super elongation complex family of RNA polymerase II elongation factors: gene target specificity and transcriptional output. Mol. Cell. Biol. 32: 2608–2617. https://doi.org/10.1128/MCB.00182-12

Luo, Z., C. Lin, and A. Shilatifard, 2012b The super elongation complex (SEC) family in transcriptional control. Nat. Rev. Mol. Cell Biol. 13: 543–547. https://doi.org/10.1038/nrm3417

Maier W., K. Moos, M. Seifert, and R. Baumeister, 2014 MiModD - Mutation Identification in Model Organism Genomes. [Computer Software]: http://SourceForge.net; 2014. 0.1.8:[Available from: https://sourceforge.net/projects/mimodd/.]. 2014.

Maxwell, C. S., W. S. Kruesi, L. J. Core, N. Kurhanewicz, C. T. Waters *et al.*, 2014 Pol II docking and pausing at growth and stress genes in C. elegans. Cell Rep. 6: 455–466. https://doi.org/10.1016/j.celrep.2014.01.008

Mello, C., and Fire, A. 1995. DNA transformation. Meth. Cell Biol. 48: 451–482.

Morimoto, R. I., 1998 Regulation of the heat shock transcriptional response: cross talk between a family of heat shock factors, molecular chaperones, and negative regulators. Genes Dev. 12: 3788–3796. https://doi.org/10.1101/gad.12.24.3788

Morley, J. F., and R. I. Morimoto, 2004 Regulation of longevity in Caenorhabditis elegans by heat shock factor and molecular chaperones. Mol. Biol. Cell 15: 657–664. https://doi.org/10.1091/mbc.e03-07-0532

Morton, E. A., and T. Lamitina, 2013 Caenorhabditis elegans HSF-1 is an essential nuclear protein that forms stress granule-like structures following heat shock. Aging Cell 12: 112–120. https://doi.org/10.1111/acel.12024

Mück, F., S. Bracharz, and R. Marschalek, 2016 DDX6 transfers P-TEFb kinase to the AF4/AF4N (AFF1) super elongation complex. Am. J. Blood Res. 6: 28–45.

Nakai, K., and P. Horton, 1999 PSORT: a program for detecting sorting signals in proteins and predicting their subcellular localization. Trends Biochem. Sci. 24: 34–36. https://doi.org/10.1016/S0968-0004(98)01336-X

Pimentel, H., N. L. Bray, S. Puente, P. Melsted, and L. Pachter, 2017 Differential analysis of RNA-seq incorporating quantification uncertainty. Nat. Methods 14: 687–690. https://doi.org/10.1038/nmeth.4324

Porta-de-la-Riva, M., L. Fontrodona, A. Villanueva, J. Cerón, 2012 Basic *Caenorhabditis elegans* methods: synchronization and observation. J. Vis. Exp. 64: e4019, https://doi.org/10.3791/4019.

Potter, S. C., A. Luciani, S. R. Eddy, Y. Park, R. Lopez *et al.*, 2018 HMMER web server: 2018 update. Nucleic Acids Res. 46: W200–W204. https://doi.org/10.1093/nar/gky448

Qi, S., Z. Li, U. Schulze-Gahmen, G. Stjepanovic, Q. Zhou *et al.*, 2017 Structural basis for ELL2 and AFF4 activation of HIV-1 proviral transcription. Nat. Commun. 8: 14076. https://doi.org/10.1038/ncomms14076

Richter, K., M. Haslbeck, and J. Buchner, 2010 The heat shock response: life on the verge of death. Mol. Cell 40: 253–266. https://doi.org/10.1016/j.molcel.2010.10.006

Saunders, A., L. J. Core, and J. T. Lis, 2006 Breaking barriers to transcription elongation. Nat. Rev. Mol. Cell Biol. 7: 557–567. https://doi.org/10.1038/nrm1981

Schindelin, J., I. Arganda-Carreras, E. Frise, V. Kaynig, M. Longair *et al.*, 2012 Fiji: an open-source platform for biological-image analysis. Nat. Methods 9: 676–682. https://doi.org/10.1038/nmeth.2019

Schulze-Gahmen, U., and J. H. Hurley, 2018 Structural mechanism for HIV-1 TAR loop recognition by Tat and the super elongation complex. Proc. Natl. Acad. Sci. USA 115: 12973–12978. https://doi.org/10.1073/pnas.1806438115

Schulze-Gahmen, U., H. Upton, A. Birnberg, K. Bao, S. Chou *et al.*, 2013 The AFF4 scaffold binds human P-TEFb adjacent to HIV Tat. eLife 2: e00327. https://doi.org/10.7554/eLife.00327

Shim, E. Y., A. K. Walker, Y. Shi, and T. K. Blackwell, 2002 CDK-9/cyclin T (P-TEFb) is required in two postinitiation pathways for transcription in the C. elegans embryo. Genes Dev. 16: 2135–2146. https://doi.org/10.1101/gad.999002

Simonis, N., J.-F. Rual, A.-R. Carvunis, M. Tasan, I. Lemmens *et al.*, 2009 Empirically controlled mapping of the Caenorhabditis elegans protein-protein interactome network. Nat. Methods 6: 47–54. https://doi.org/10.1038/nmeth.1279

Sims, R. J., R. Belotserkovskaya, and D. Reinberg, 2004 Elongation by RNA polymerase II: the short and long of it. Genes Dev. 18: 2437–2468. https://doi.org/10.1101/gad.1235904

Stan Development Team, 2018. *PyStan: the Python interface to Stan*, Version 2.17.1.0. http://mc-stan.org.

Van Buskirk, C., and P. W. Sternberg, 2007 Epidermal growth factor signaling induces behavioral quiescence in *Caenorhabditis elegans*. Nat. Neurosci. 10: 1300–1307. https://doi.org/10.1038/nn1981

van der Walt, S., J. L. Schönberger, J. Nunez-Iglesias, F. Boulogne, J. D. Warner *et al.*, 2014 scikit-image: image processing in Python. PeerJ 2: e453. https://doi.org/10.7717/peerj.453

Voellmy, R., and F. Boellmann, 2007 Chaperone Regulation of the Heat Shock Protein Response, pp. 89–99 in *Molecular Aspects of the Stress Response: Chaperones, Membranes and Networks*, *Advances in Experimental Medicine and Biology*. edited by P. Csermely, L. Vígh, Springer, New York.

Wang, H., J. Liu, S. Gharib, C. M. Chai, E. M. Schwarz *et al.*, 2017 cGAL, a temperature-robust GAL4–UAS system for *Caenorhabditis elegans*. Nat. Methods 14: 145–148. https://doi.org/10.1038/nmeth.4109

Wang, H., H. Park, J. Liu, and P. W. Sternberg, 2018 An efficient genome editing strategy to generate putative null mutants in Caenorhabditis elegans using CRISPR/Cas9. G3: genes, genomes. Genetics 8: 3607–3616. https://doi.org/10.1534/g3.118.200662

Zhou, Q., T. Li, and D. H. Price, 2012 RNA polymerase II elongation control. Annu. Rev. Biochem. 81: 119–143. https://doi.org/10.1146/annurev-biochem-052610-095910

Communicating editor: M. Sundaram